Twelve-hour tides in the winter northern polar mesosphere and lower thermosphere

Genene M. Fisher,[1,2] Richard J. Niciejewski,[1] Timothy L. Killeen,[3] William A. Gault,[4] Gordon G. Shepherd,[4] Stephen Brown,[5] and Qian Wu[3]

[1]   An investigation of the tidal oscillations near the winter northern polar mesopause has been carried out at Resolute Bay, Canada (74.9°N, 94.9°W). The daily, monthly, and annual variations of the tidal field were studied using the 1995/1996 and 1996/1997 data. Ground-based measurements were obtained using a Fabry-Perot interferometer with a circle to line interferometric optical system (FPI/CLIO) and the E Region Wind Interferometer (ERWIN). The FPI/CLIO observed the Doppler winds of the OH emission near 86 km altitude. The ERWIN provided simultaneous OH (near 86 km) and OI (near 97 km) wind measurements. Monthly data were compared to the Global Scale Wave Model (GSWM) and the Forbes/Vial Solar Semidiurnal Tidal Model predictions. Analysis of the 12-hour oscillation near 86 and 97 km altitudes indicates that it is persistent and characteristic of a semidiurnal propagating tide. The semidiurnal tide was found to be highly variable in amplitude and phase from day to day. The observations presented provide a continuous and extensive data set for the winter season.   *INDEX TERMS:* 3332 Meteorology and Atmospheric Dynamics: Mesospheric dynamics; 3334 Meteorology and Atmospheric Dynamics: Middle atmosphere dynamics (0341, 0342); 3384 Meteorology and Atmospheric Dynamics: Waves and tides; *KEYWORDS:* Semidiurnal tide, polar mesosphere, polar thermosphere, Fabry-Perot interferometer, Resolute Bay, mesopause

1. Introduction

[2]   The upper mesosphere/lower thermosphere (MLT) is a complex region dominated by a mixture of propagating tides, gravity waves, planetary waves and in-situ forcing from solar heating. Measurements in the northern high latitudes have resulted in various interpretations involving reference to inertio-gravity waves, zonally symmetric tides, pseudotides, and non-linear interactions between waves [*Sivjee et al.*, 1994; *Forbes et al.*, 1995; *Walterscheid and Sivjee*, 1996; *Oznovich et al.*, 1997]. Currently this region is still the least understood of all the atmospheric regions, mostly due to the difficulty in obtaining diagnostic measurements. Observations at the northern polar latitudes are sparse due to the lack of ground-based instruments at suitable sites and appropriately-instrumented satellites with high orbital inclination. There exist only a few works that address the dynamics of the neutral MLT in the northern polar region— research has focused on observations at Resolute (74.9°N,

94.9°W) [*Fisher et al.*, 1999, 2000] and Eureka (80°N, 85°W) [*Sivjee et al.*, 1994; *Oznovich et al.*, 1995; *Walterscheid and Sivjee*, 1996; *Oznovich et al.*, 1997].

[3]   There has been more research published using southern polar MLT measurements, including work by *Hernandez et al.* [1992a, 1992b, 1993, 1996]; *Sivjee and Walterscheid* [1994]; *Forbes et al.* [1995, 1999]; *Portnyagin et al.* [1998, 2000]; and *Walterscheid and Sivjee* [2001]. Many of these studies have shown that the flow near the geographic pole is characteristic of zonal wave number 1, while scalar variables, such as temperature and emission rates are of zonal wave number 0. As a result, observed 12 h waves in the wind measurements are not believed to be from a tidal source.

[4]   However, in the northern polar regions, more research is needed to assess the climatology and determine the mechanisms to explain the complex observations. This study obtains and analyzes such data in order to characterize the waves found in the northern polar regions. The experimental investigation uses optical instrumentation at the Resolute Bay Observatory facility at Resolute Bay, Canada (74.9°N, 94.9°W) to observe the OH and OI airglow emissions. Many authors have reported the OH emission peak altitude to be between 80–90 km [*Baker and Stair*, 1988; *Lopez-Moreno et al.*, 1987]. In this paper, we refer to 86 km as the mean OH peak height. The atomic oxygen (green line) emission peak is generally accepted to be near 97 km [*Greer et al.*, 1986]. This paper provides long-term (entire season) observations of the mesosphere and lower thermosphere winds in the northern polar cap for two years. The Global Scale Wave Model [*Hagan et al.*, 1999] and the Forbes/Vial Solar Semidiurnal Tidal Model [*Forbes and*

---

[1]Space Physics Research Laboratory, University of Michigan, Ann Arbor, Michigan, USA.

[2]Now at Atmospheric Policy Program, American Meteorological Society, Washington, D. C., USA.

[3]National Center for Atmospheric Research, Boulder, Colorado, USA.

[4]Centre for Research on Earth and Space Sciences, York University, Toronto, Ontario, Canada.

[5]Centre for Research in Earth and Space Technology, Toronto, Ontario, Canada.
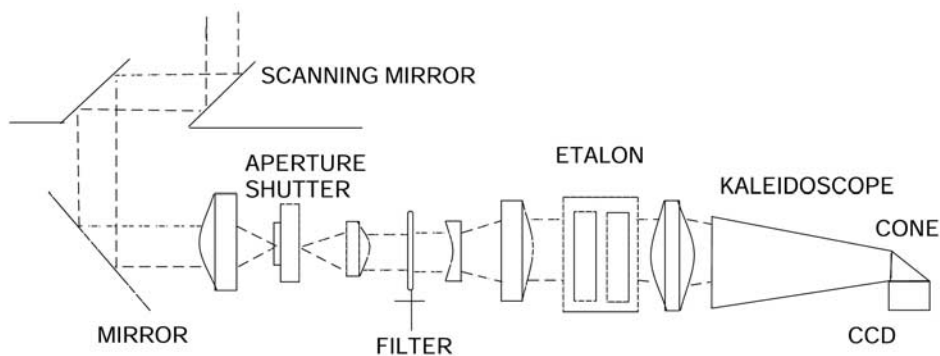
Figure 1.   General layout of the FPI/CLIO at Resolute.

Vial, 1989] analyses are compared to the ground-based observations.

2.   Instrumentation

[5] Polar cap mesospheric winds observed with a Fabry-Perot interferometer with a circle to line interferometric optical system (FPI/CLIO) have been compared with measurements from a field-widened Michelson interferometer optimized for *E* region winds (ERWIN). *Fisher et al.* [1999] presented the first FPI/CLIO mesopause wind results above Resolute. *Fisher et al.* [2000] showed that both optical techniques provide equivalent observations of the mesopause winds at Resolute.
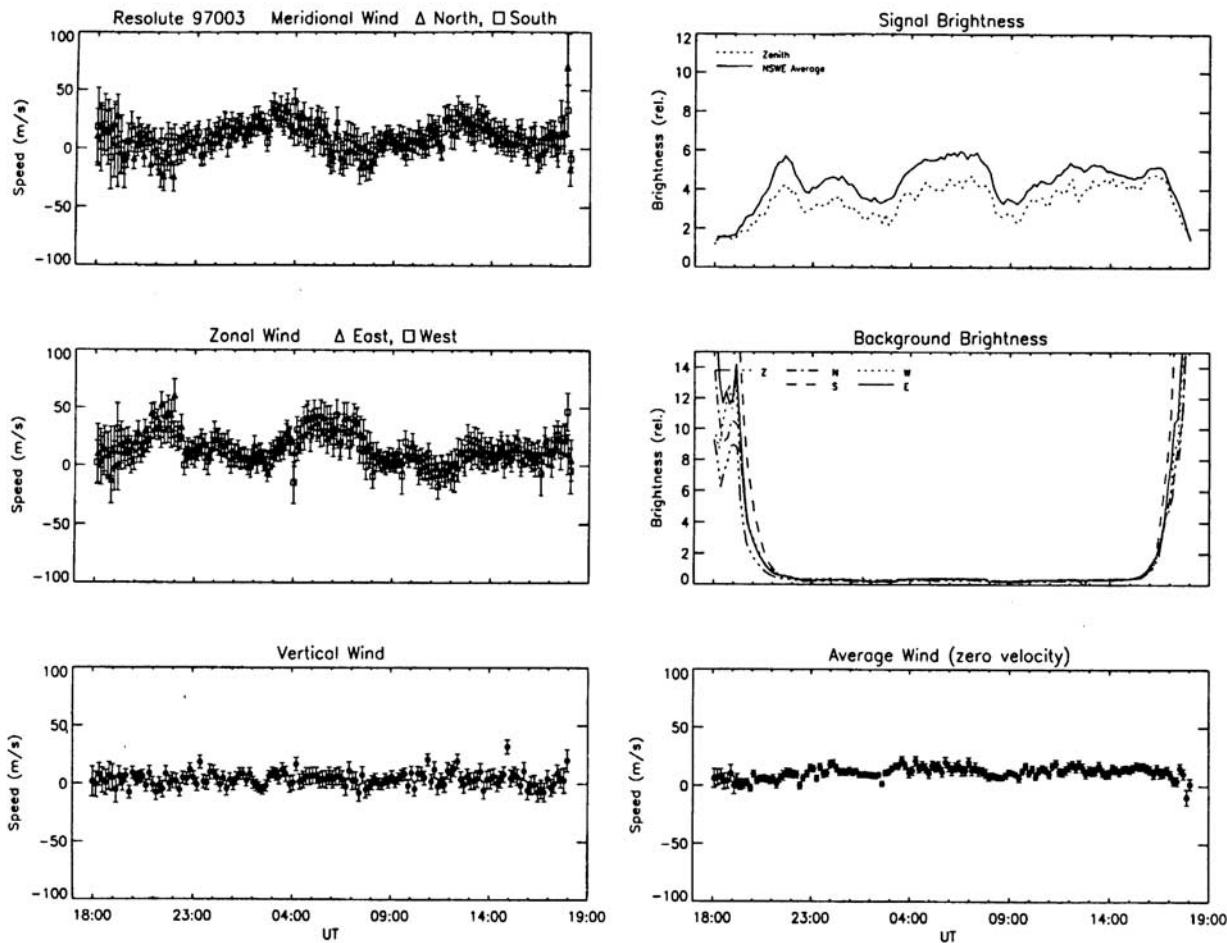

Figure 2.   The geophysical parameters calculated for January 4, 1997 (also represented by Day 97003) using the FPI/CLIO.
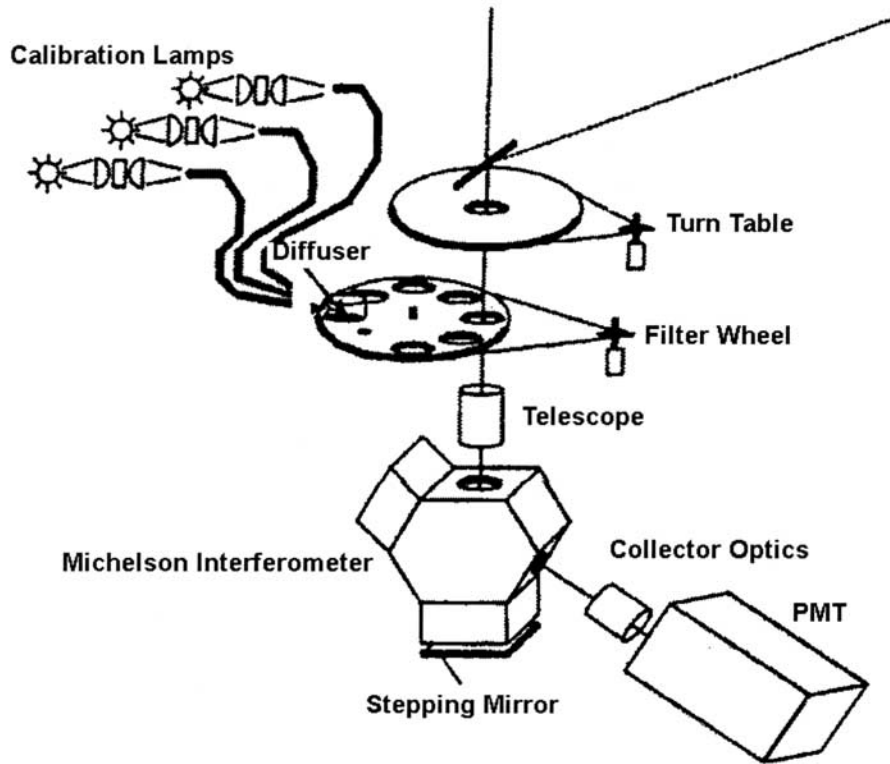
Figure 3. General layout of ERWIN. PMT, photomultiplier detector.

2.1. University of Michigan Fabry-Perot Interferometer With a Circle to Line Interferometric Optical System
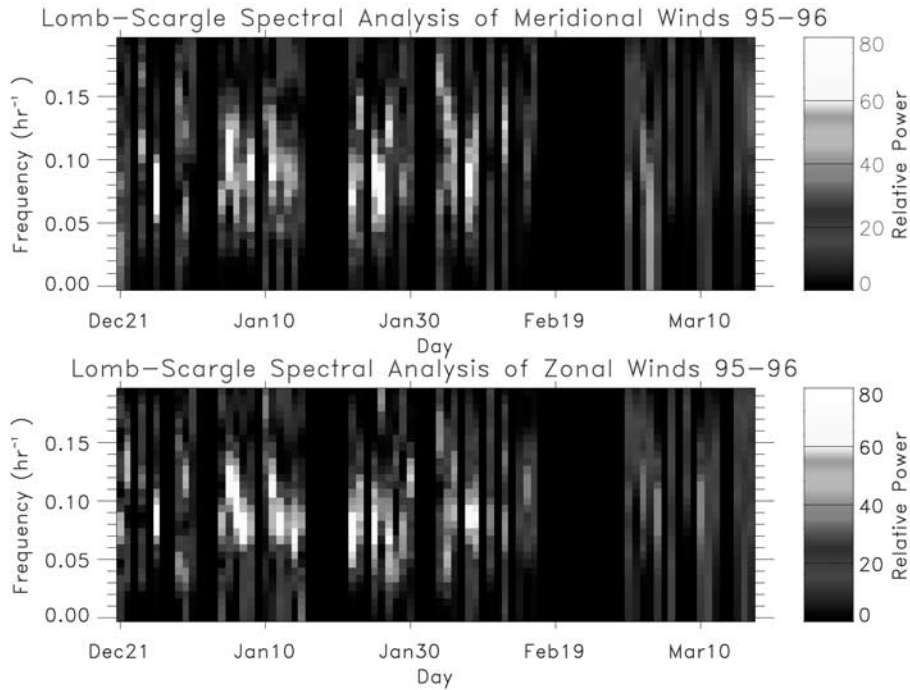
[6] The FPI used at Resolute Bay consists of a circle to line interferometric optical system. The general layout is found in Figure 1. This novel technique converts the circular Fabry-Perot interferometric fringe pattern into a linear array [*Hays*, 1990]. The FPI/CLIO field of view (2.86°) allows approximately 9 orders of the OH (7, 3) emission to be collected simultaneously by the CCD. The etalon diameter is 15 cm and has a 9.6 cm clear aperture. The etalon has a reflectivity finesse of 20 and the 2 cm gap overlaps the OH(7, 3)P_1(3) doublet. The optical measurements are made in the four cardinal directions at an elevation of 45° above the horizon and in the zenith. The 45° angle allows for measurements of the OH airglow at 86 km away from the station. The FPI/CLIO performs a 90 second integration in each direction, taking less than 10 minutes for a full scan. The average FPI/CLIO measurement error, derived from the OH spectrum by a non-linear least squares fit, is about 8 m/s. The laboratory performance of the FPI/CLIOInstrument is described by *Wu et al.* [1994] while a detailed description of the CLIO system is given by *Hays* [1990].

[7] The CLIO system consists of (1) an f/10 achromatic doublet lens with a focal length of 150 cm, (2) two first-surface float glass mirrors that form a 90° kaleidoscope (V-mirror), and (3) a 45 degree conical mirror diamond-turned in aluminum. The optical conversion is accomplished by using a 45-degree reflective cone to convert the rings into a series of short line segments onto the optical axis. This setup by itself only allows one quarter of each ring to fall onto the detector, while three fourths of the signal is lost. Inserting a mirrored kaleidoscope recaptures the lost signal. The function of the kaleidoscope is to fold the circular FPI fringe pattern into the quadrant of the focal plane occupied by the cone. The resulting 90-degree fringe arcs are then converted to line segments on the CCD by reflection from the conical mirror. Each channel of the CCD (about 200–240 pixels) is binned into one super pixel.

[8] FPI/CLIO wind measurements discussed in this paper were obtained continuously throughout the months of December-March 1995/1996 and 1996/1997. Figure 2 is an example of the output measurements obtained with the FPI/CLIO on January 4, 1997 (Day 97003). Note that the instrument software assumes January 1 to be Day 000. On the left side, the top and middle panel show the meridional and zonal wind measurements, respectively. The bottom left panel shows the vertical wind (zenith measurement). The top right panel shows signal brightness with the zenith and North-South-West-East average brightnesses plotted. The middle right plot shows the background brightness with the zenith and North-South-West-East average brightnesses plotted. The bottom right panel shows the average wind (average of a cycle of measurements in the zenith

Figure 4. The geophysical parameters calculated for December 26, 1995 using ERWIN. The top three panels show the vector winds for the OI, O$_2$, and OH emissions, respectively. The bottom two show the intensity and visibility plots, respectively. The solid line is the OI emission, the dashed line is the O$_2$ emission, and the dotted line is the OH emission.

and four cardinal directions) which is used as the zero velocity reference. The meridional wind is defined as positive to the northward direction and the zonal wind is defined as positive to the eastward direction. It takes less than 10 minutes for a scan in the sequence zenith, north, south, west, east, and background. It takes about 1.8 minutes between north and south or between west and east measurements.

Figure 5. Lomb Scargle spectral analysis on the FPI/CLIO OH (7, 3) (892.0 nm) winds is performed for each day in 1995/1996 using a maximum frequency of 0.2/h and then plotted in a time series. Cloudy days were not analyzed, and no data are plotted for those days.

2.2. York University *E* Region Wind Interferometer

[9] The *E* Region Wind Interferometer (ERWIN) is a field-widened Michelson interferometer designed to measure upper atmosphere winds using the three emissions: OI (557.7 nm), OH (6, 2) $P_1(3)$ (843.0 nm), and O_2 (0, 1) (866.0 nm). ERWIN has been described by *Gault et al.* [1996]. The layout of the instrument is shown in Figure 3.
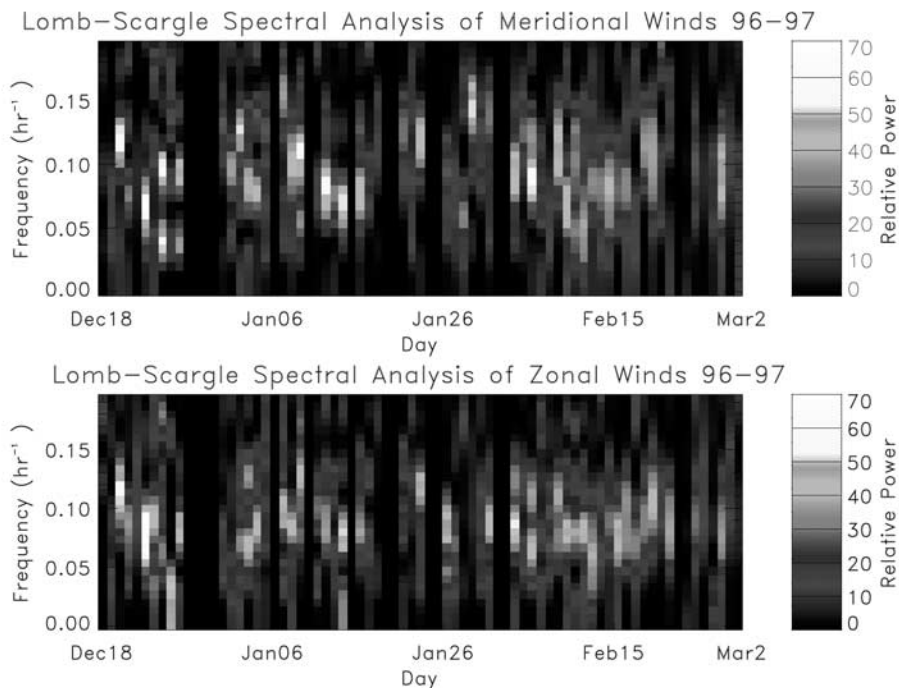
Figure 6. Same as Figure 5, but for the 1996/1997 season.
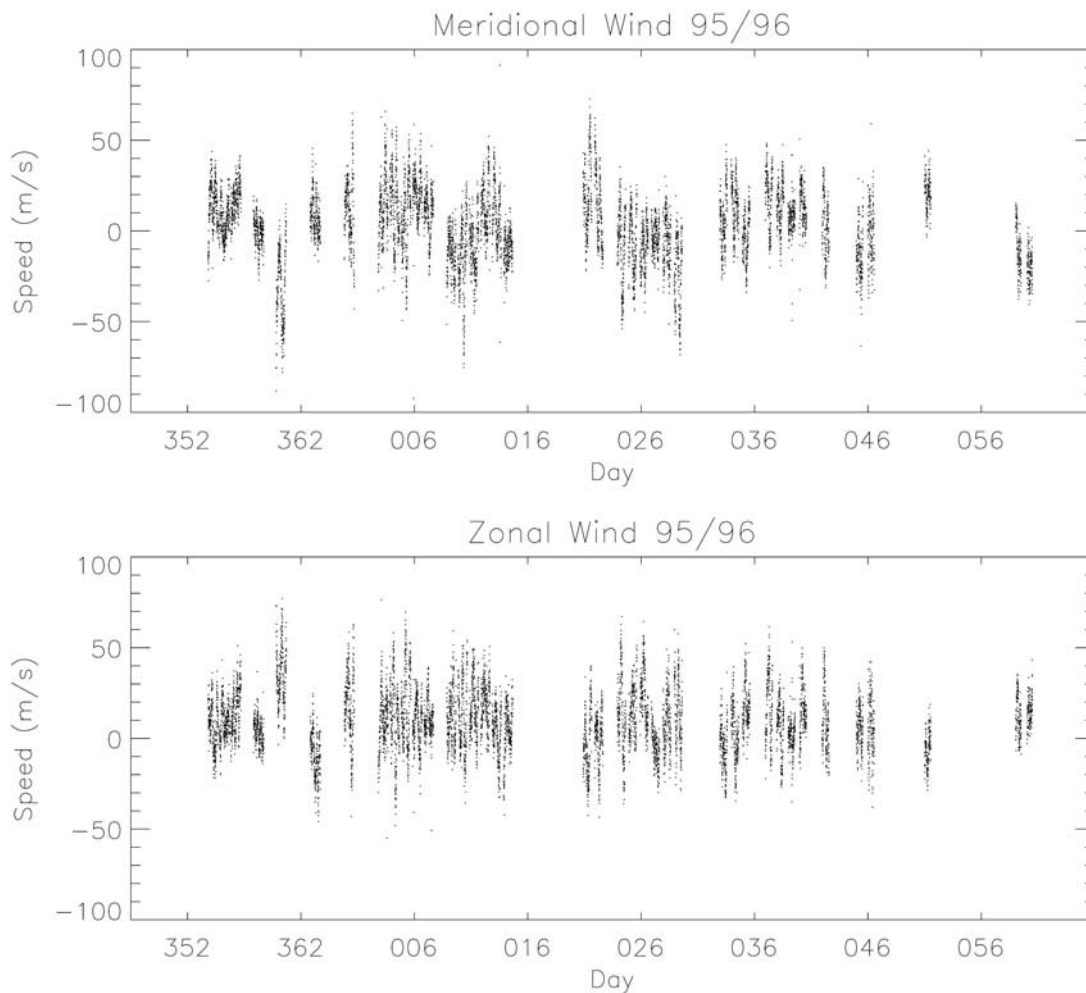
Figure 7. OH meridional (top) and zonal (bottom) winds for the 1995/1996 observing season. Cloudy days were removed. Measurements were taken with the FPI/CLIO at Resolute.

[10] The reflective mirrors in ERWIN are set to an optical path difference of 11 cm to suppress the fringe from the hot F region emission of OI and measurements of visibility are taken at only that path difference. Field widening and thermal compensation are achieved over the large spectral range by the use of three types of glass in the interferometer's arms. An Argon lamp at 866.7 nm is used to calibrate the OH(6,2) emission and a Krypton lamp at 557.0 nm is used to calibrate the OI emission. The zero wind is determined from the average of the four cardinal directions.

[11] The measurements are made at 30° elevation in four azimuths displaced from the cardinal directions by 17° in the positive azimuth sense. The 30° angle allows for measurements of the OH airglow at 149 km from the station in these directions.

[12] ERWIN wind measurements discussed in this paper were obtained continuously throughout the months of November-February during 1995/1996 and 1996/1997. Figure 4 is an example of the vector winds, intensity, and visibility measurements obtained with ERWIN on December 26, 1995. The meridional wind is defined as positive to

the north and the zonal wind is defined as positive to the east. Visibility is the ratio of the amplitude of the modulation produced by the Michelson to the average value of the signal. Measurement accuracy is ~4 m/s. A scan takes 3.6 minutes when observing only one emission in the four cardinal directions without zenith measurements. Otherwise, it takes 20 minutes for a scan in the four cardinal directions for each emission, zenith for each emission, and then phase calibrations using three wavelength-specific lamps.

3. Data Analysis

[13] A limitation in the observations made by any ground-based interferometer is the presence of clouds. At Resolute, cloud cover conditions in tenths are recorded every hour by the Canadian Meteorological Centre of Environment Canada. These records are used to eliminate data taken by the instrument during overcast skies. During cloudy conditions, there is no difference between the zenith and NSWE average signal brightnesses and the wind amplitude is typically zero. The OH brightness measured
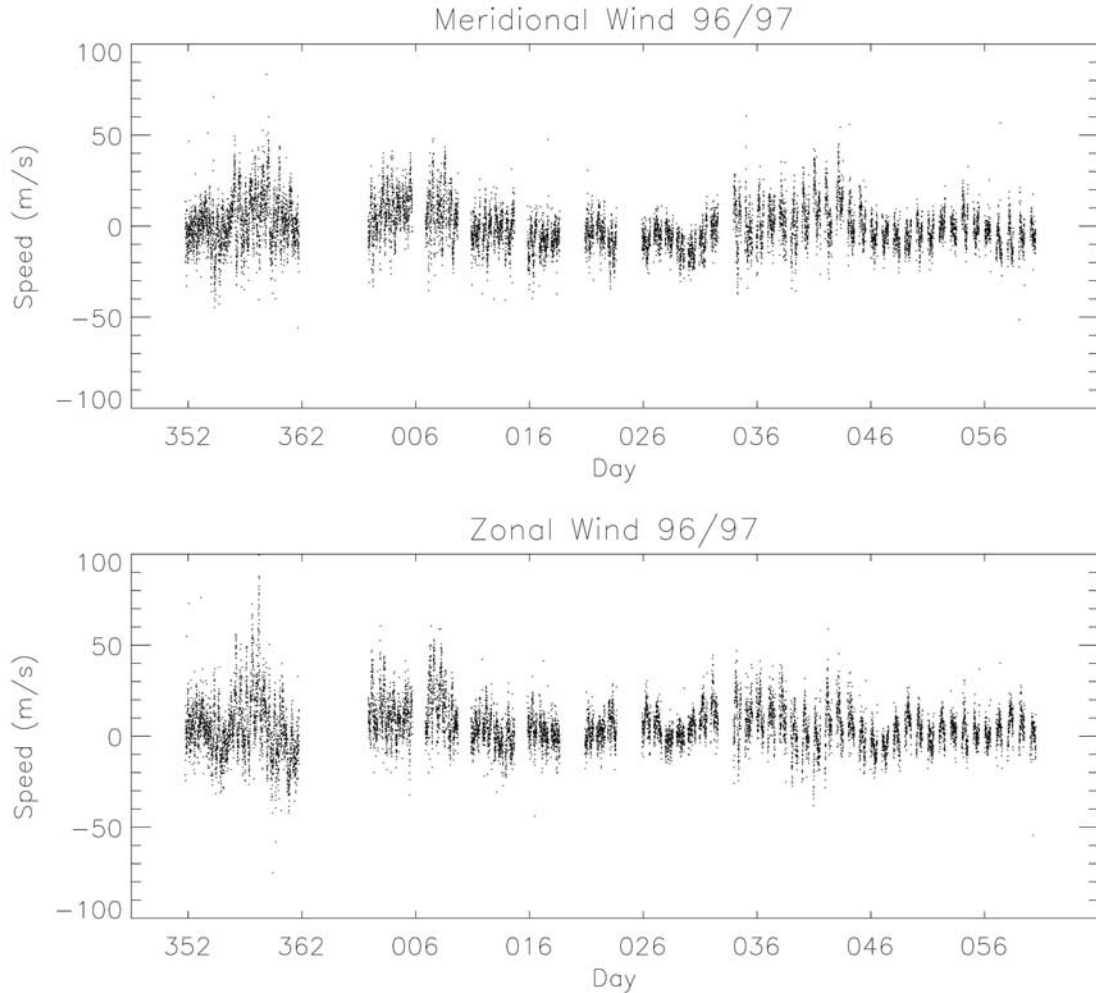
Figure 8. OH meridional (top) and zonal (bottom) winds for the 1996/1997 observing season. Cloudy days were removed. Measurements were taken with the FPI/CLIO at Resolute.

at 45 degrees from the station should be greater than the zenith measurement as a result of the Van Rhijn Enhancement. On cloudy days, the brightness ratio is equal to 1 and the resulting wind speed is 0 m/s. These effects seen in the observations are indirect indicators that clouds exist in the field of view of the instrument during the measurements. A clear night was characterized as having less than 4/10 cloud cover for more than half of the night. In the 1995/1996 data set there were 50 relatively clear nights and in the 1996/1997 data set there were 61 relatively clear nights.

[14] The Resolute wind measurements are unevenly spaced and range less than 24 hours a day. During December about 23 hours of data are obtained while during March only 8 hours are available since nightglow studies are limited by the duration of the nocturnal window. Interpretations of wind measurements can be complicated by sampling and aliasing issues. Data gaps can introduce artificial frequencies in the data analysis. Consideration must be given to these issues when analyzing a data set.

[15] The first step in analysis was to perform a least squares fit for each horizontal component for each day.

Values of mean wind, amplitude, period, and phase can be represented mathematically by

$$F(x) = A_o + A_1\cos(\omega_1 t + \varphi)$$

where ω_1 is the frequency (i.e. $2\pi/12$ is the semidiurnal frequency), A_o is the mean, A_1 is the amplitude of the oscillation, t is time, and φ is the phase value representing the local time maximum eastward or northward flow for the oscillation. In this paper, the mean wind, also referred to as the background wind, is defined as the offset from 0 m/s. The data showed that the 12 h oscillation is the dominant wave, so each day of data was fit with a fixed 12 h period. This analysis was performed on each individual day since the data gaps between some days spanned from a few hours to a day. Also, the phase of the 12 h tide can vary from day to day and a single least squares fit could not properly fit more than a few days at a time.

[16] The second stage of analysis involved using the Lomb-Scargle spectral analysis technique [*Press et al.*, 1992]. The Lomb-Scargle method performs a spectral analysis on unevenly sampled data and can test the signifi-
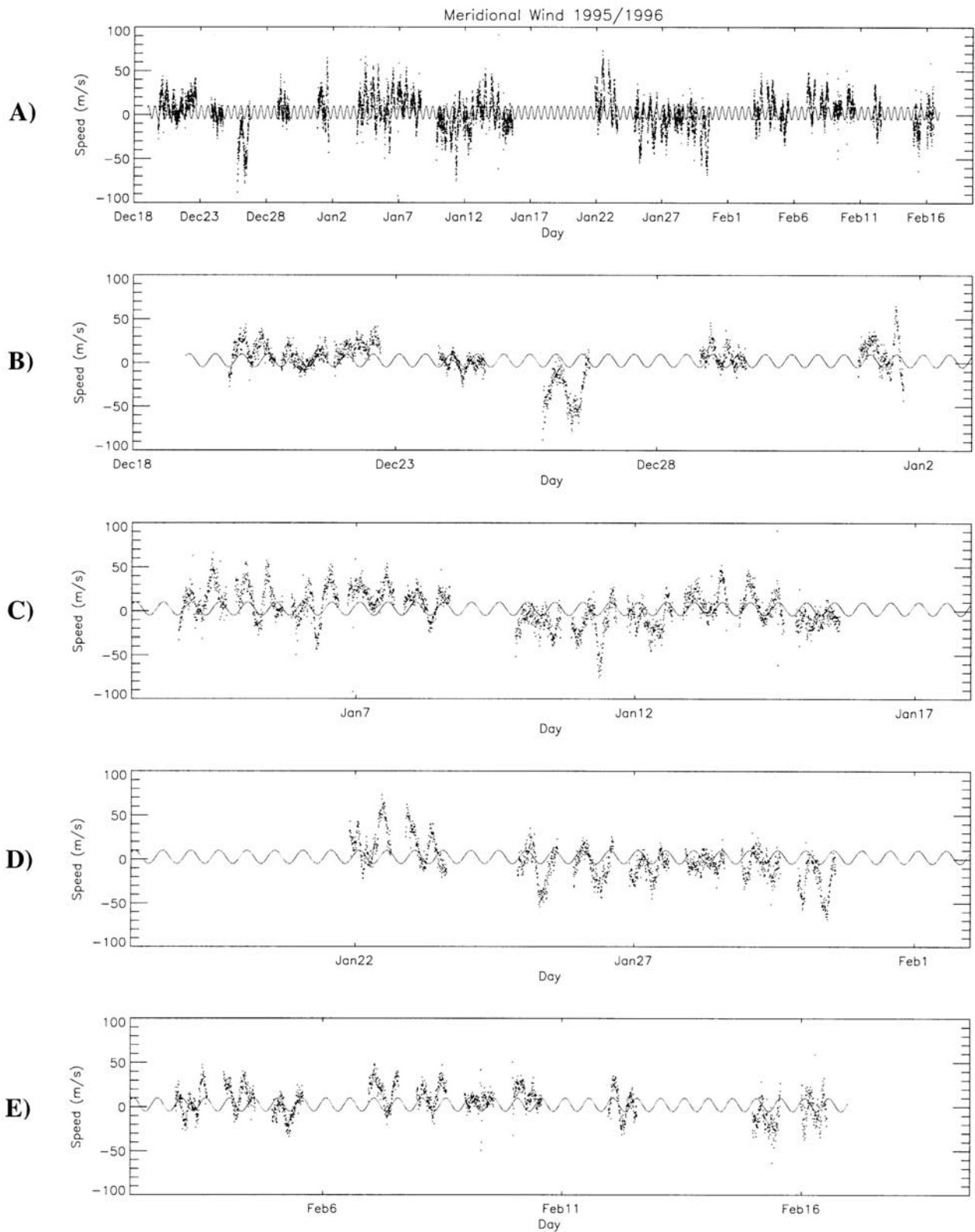
Figure 9. Meridional FPI/CLIO OH (892.0 nm) winds during 1995/1996. The top plot (A) shows the winds from December 20, 1995 to February 16, 1996. A detailed view is shown during B) Dec 20–Jan 1, C) Jan 4–Jan 15, D) Jan 22–Jan 30, and E) Feb 3–Feb 16. The least squares fit shown has an amplitude of 7.69 ± 0.8 m/s, background wind of 2.4 ± 0.5 m/s, and a phase of 2.8 ± 0.2 h.
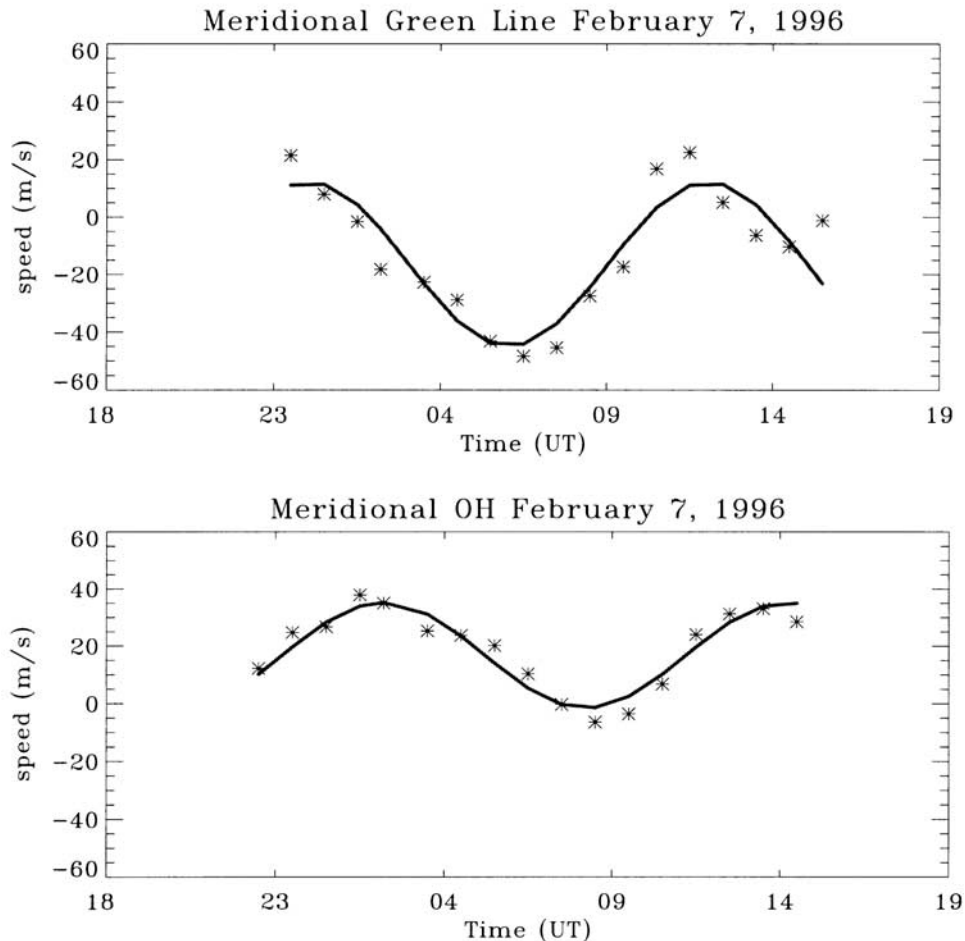
Figure 10. An example of a 12 h propagating wave. A least squares cosine fit with a fixed 12 h period (solid line) is plotted over the wind data (asterisks). The top plot shows ERWIN OI (green line) winds ($\sim$97 km) with an amplitude of 28.6 ± 1.4 m/s, a background wind of -16.4 ± 1.0 m/s, and a phase of -0.3 ± 0.4 h. The bottom plot shows FPI/CLIO OH winds ($\sim$86 km) with an amplitude of 18.3 ± 1.4 m/s, a background wind of 16.8 ± 1.0 m/s, and a phase of 2.5 ± 0.4 h.

cance of periodic signals. This method also calculates the false alarm probability of a periodic signal. The Lomb-Scargle analysis has been an accepted tool in the aeronomy field for analyzing unevenly sampled data [e.g., *Manson et al.*, 1998; *Salah et al.*, 1997; *Forbes and Zhang*, 1997; *Oznovich et al.*, 1997; *Hernandez et al.*, 1993].

## 4. Daily Variability of the Semidiurnal Tide

[17] Wind measurements taken at Resolute show daily wave variability, with the 12 h oscillation evident in both the meridional and zonal winds. To search for tidal oscillations, a Lomb-Scargle spectral analysis for unevenly sampled data [*Press et al.*, 1992] was performed for each of the clear nights. Figure 5 is a contour plot showing the individual Lomb-Scargle analyses for each night plotted in a time series during the 1995/1996 observing season. Figure 6 shows the same results for the 1996/1997 season. Strong spectral peaks between 12 h (0.83 h^{-1}) and 8 h (0.125 h^{-1}) are frequently observed in the data. However, the spectral peaks are not "locked in" at specific frequencies, but rather show significant daily variability throughout the three months. The spectral power is stronger in January than in March, but that

may be due to the fewer number of measurements taken as the equinox approaches. The limiting frequency in December is 0.04 h^{-1} (23 h) while it steadily increases throughout the data until March when it is 0.125 h^{-1} (8 h).

5. Long-Term Variability

[18] The entire season of FPI/CLIO OH wind data for 1995/1996 is presented in Figure 7. These measurements were obtained between December and March. Figure 8 shows the OH winds observed during the 1996/1997 season. Cloudy days were removed in both figures. Both years show variability in the data. The mean wind appears to vary throughout the season. The amplitude of both the meridional and zonal wind also appears to fluctuate. The winds during the 1995/1996 season tend to show larger amplitudes than during 1996/1997. Long-term variations, on the order of days, appear to be modulating the semidiurnal characteristics.

[19] The semidiurnal tide at Resolute is variable in phase and amplitude. To demonstrate this behavior, a least squares fit with a fixed 12 h period is plotted over the 1995/1996 meridional data (Figure 9). The top plot in Figure 9 shows the data from December 20, 1995 to February 16, 1996.
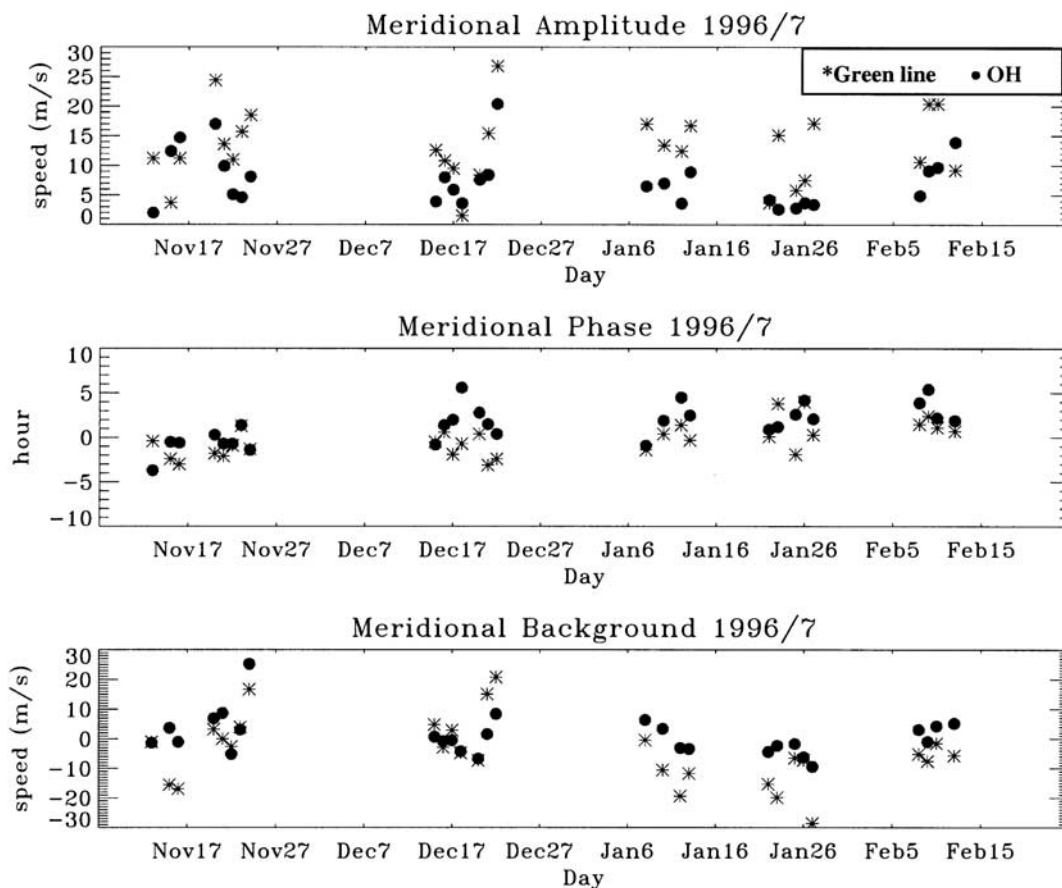
Figure 11. The top panel shows 12 h least squares fit amplitude results for the meridional winds during 1996/1997. The middle plot shows phase values and the bottom plot shows background (offset) values. The OH data are marked with solid circles and the OI (green line) data are marked with asterisks. The errors are ∼1.4 m/s for amplitude, ∼0.3 h for phase, and ∼1.0 m/s for background wind. The OI (green line) data were obtained from ERWIN and the OH data were obtained from ERWIN during November and from FPI/CLIO during December–February.

Each subsequent plot shows a detailed look at a segment of time between those two dates. It is clear from this plot that the mean wind and semidiurnal phase and amplitude varies considerably throughout the season. This is evident in the winds during January 4–8. While the least squares fit does not agree with the wind data between January 4–6, the fit does a good job of representing the phase between January 7–8. Basically this shows that the phase can vary over a short range. This variability can be due to effects such as planetary waves interacting with the global tidal fields, and perhaps also creating non-migrating modes. *Manson et al.* [1999] found that the winter high-latitude tides demonstrate the highest interannual variability and are not well modeled. Similar examples of daily phase shift differences are also found throughout Figure 9. This explains why each day was analyzed individually. This also made it difficult to perform a multiple period fit when analyzing more than a day worth of data.

6. Altitudinal Analysis

[20] Simultaneous ground-based wind measurements of the OH and OI emissions have been made at Resolute Bay.

In November, the OH measurements were provided only from ERWIN. Analyses of the daily OH and OI winds show that the 12 h wave is the dominant periodic oscillation and has the characteristics of a propagating tide. Figure 10 shows an example of an upward propagating wave. Twelve hour least squares fit results show an amplitude increase with height and downward phase propagation. Westward propagating waves have a westward phase tilt (downward phase progression) when they have an upward energy progression.

[21] Daily winds were binned by hour and then fit with a least squares cosine fit with a fixed 12 h period. Results of the fit gave amplitude, phase, and background (offset) values. Figure 11 shows results for the meridional wind and Figure 12 shows the results for the zonal wind in 1996/1997. The FPI/CLIO OH data were used in the December–February analyses, while the ERWIN OH data were used in the November analyses. (ERWIN OH and OI data were available November–February, while FPI OH data were available December–March.) These results are similar for both years. The OI (green line) amplitude is usually greater than the OH amplitude. The green line amplitude peak occurs earlier than the OH amplitude peak. These behaviors are characteristic of a propagating tide. Instances when the
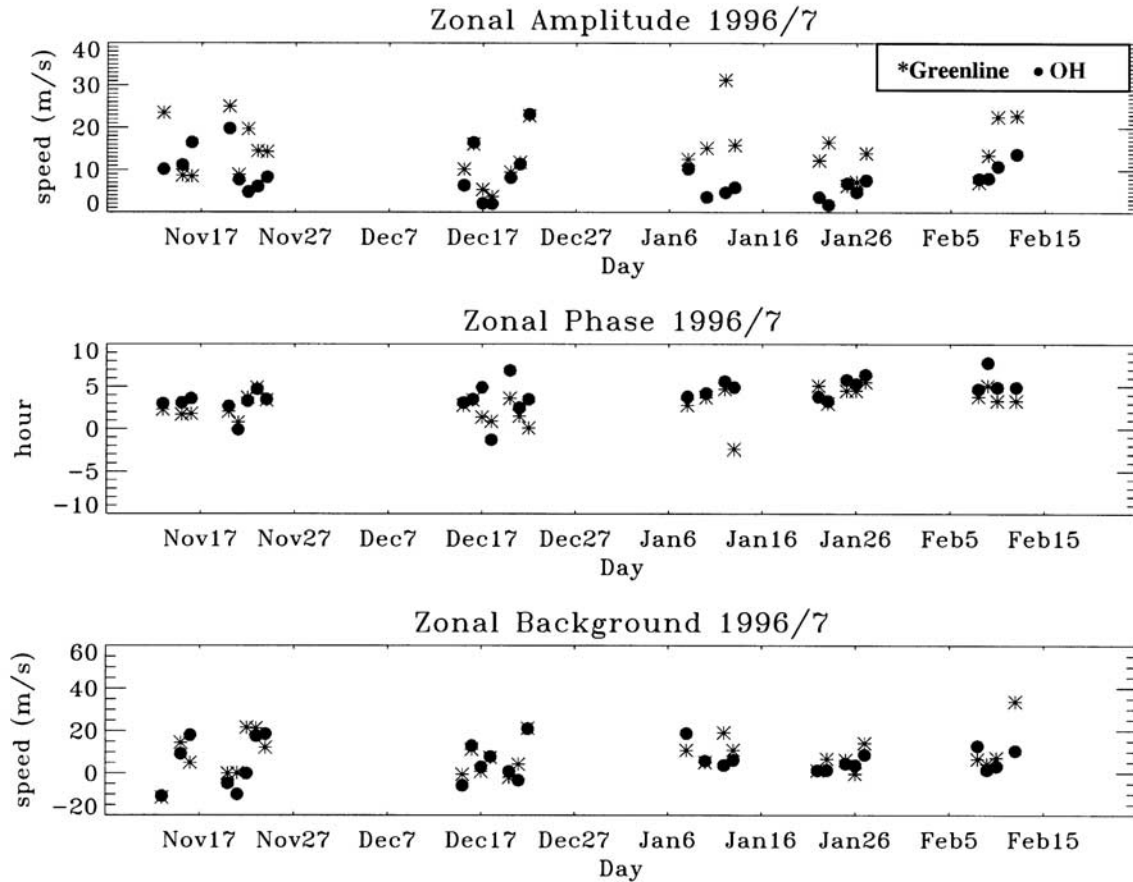
Figure 12. The top panel shows 12 h least squares fit amplitude results for the zonal winds during 1996/1997. The middle plot shows phase values and the bottom plot shows background (offset) values. The OH measurements are marked with solid circles and the OI (green line) data are marked with asterisks. The errors are ~1.4 m/s for amplitude, ~0.3 h for phase, and ~1.0 m/s for background wind. The OI (green line) data were obtained from ERWIN and the OH data were obtained from ERWIN during November and from FPI/CLIO during December–February.

OI amplitudes were smaller are attributed to the complex wind behavior near 97 km. Phase differences of less than 1.5 h between the OI and OH winds occurred when more than one wave was present.

[22] Figures 13 and 14 show monthly OH and OI (green line) amplitude comparisons between the observations and the Global Scale Wave Model (GSWM) at 75°N [*Hagan et al.*, 1999] and the Forbes/Vial Solar Semidiurnal Tidal Model (F/V) model at 74°N [*Forbes and Vial*, 1989]. The model results were obtained from the National Center for Atmospheric Research (NCAR) Coupling, Energetics, and Dynamics of Atmospheric Regions (CEDAR) database. The OH observations have amplitudes ~4 m/s greater than the model results. The OI observations have amplitudes ~10 m/s smaller than the model results.

[23] Figures 15 and 16 show monthly OH (~86 km) and OI (green line) (~97 km) phase comparisons between the observations and the GSWM at 75°N and F/V model at 74°N. The F/V model shows phase decrease with time, while the data show phase increase with time. During November, there seems to be ~3 h phase difference between the model and the observations. In general, wave mixing is more apparent during November and December.

[24] The phase lag difference between the wind determinations at the two heights of emission is a measure of the vertical wavelength of propagation of the oscillation affecting these neutral emission layers. The vertical wavelength of the 12 h wave between the OH and OI data are calculated as: (Δ altitude)*12 h/phase lag.

[25] *Hernandez et al.* [1995] did a study over 300 days at Mount John (43.98°S, 170.42°E) using the OH and OI ground based measurements and the emission heights determined from the WINDII experiment. They found that the semidiurnal tide had a typical vertical wavelength between 20–40 km, except brief periods when values reached 100 km during the fall equinox. The calculation of vertical wavelength is highly sensitive to the phase shift of the oscillations being compared. Tidal phases from Resolute have already been shown to be highly variable and slight differences can result in large calculated vertical wavelengths.

[26] Figure 17 shows that 1995/1996 monthly vertical wavelength values in the meridional component are comparable to the F/V model results except in January. The monthly values were determined by using the monthly averages of the amplitude and phase from Figures 13–16.
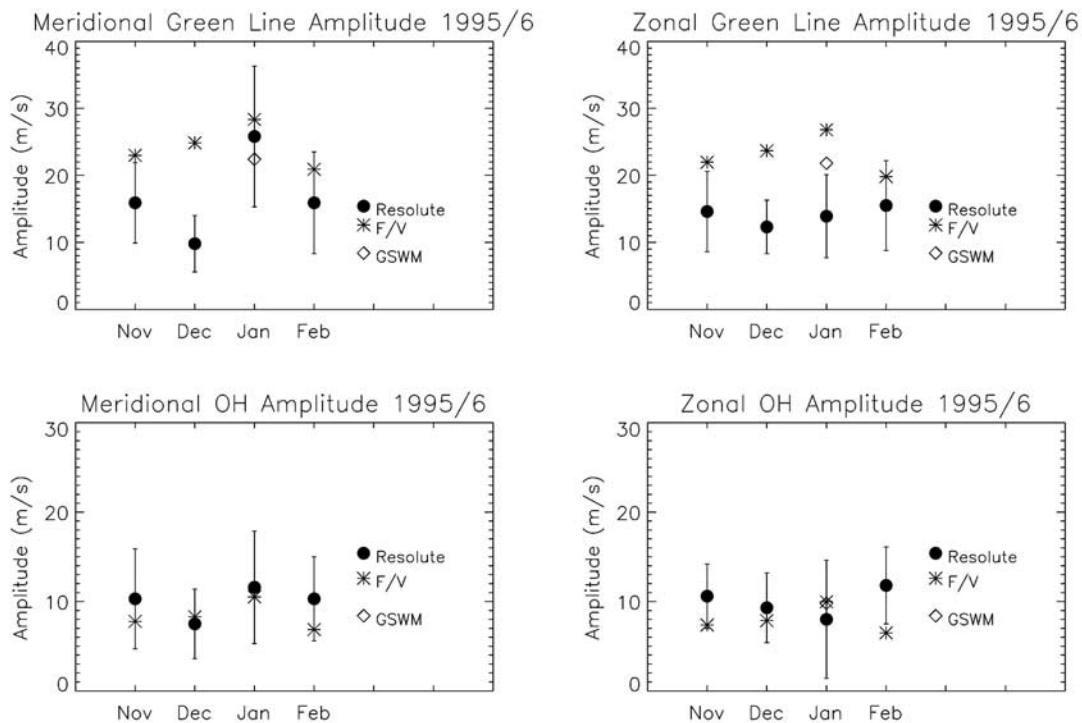
Figure 13. Monthly semidiurnal amplitudes for the 1995/1996 season. The top two plots show the OI (green line) ($\sim$97 km) meridional and zonal amplitudes and the bottom plots show the OH ($\sim$86 km) amplitudes. The Resolute data error bars are plotted. The green line measurements are compared to the Forbes/Vial (F/V) model results at 74°N at 97 km and the GSWM model results at 75°N at 98 km. The OH measurements are compared to the F/V results at 86 km and the GSWM results at 86 km. The OI (green line) data were obtained from ERWIN and the OH data were obtained from ERWIN during November and from FPI/CLIO during December–February.
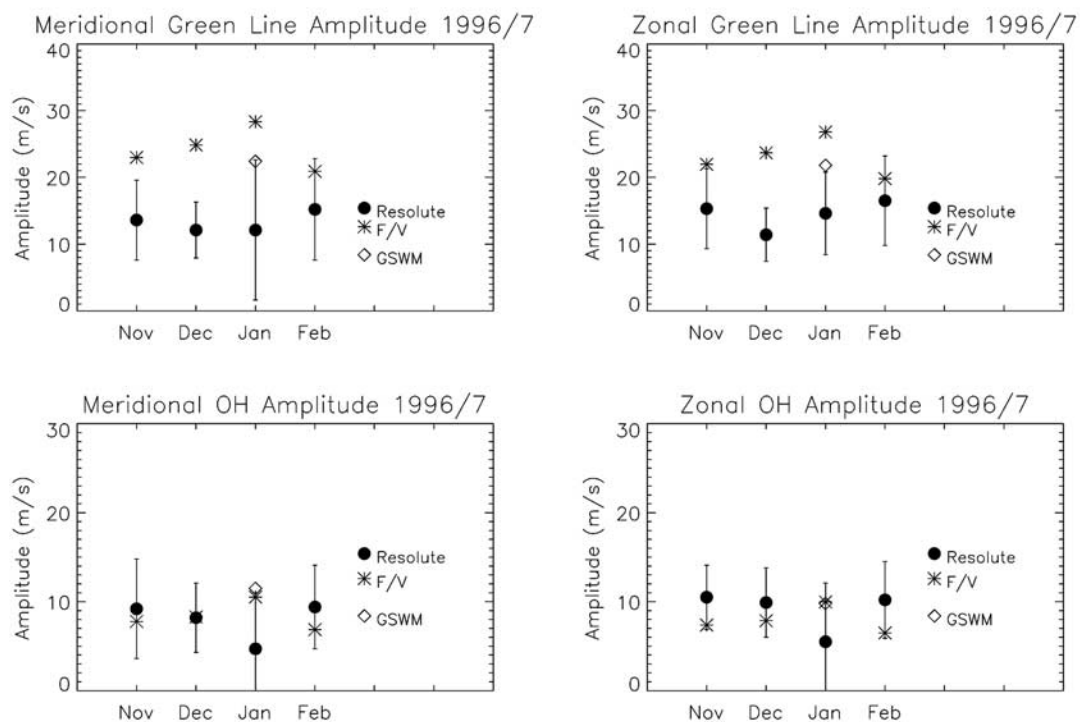

Figure 14. Same as Figure 13 but for the semidiurnal amplitudes during the 1996/1997 season.
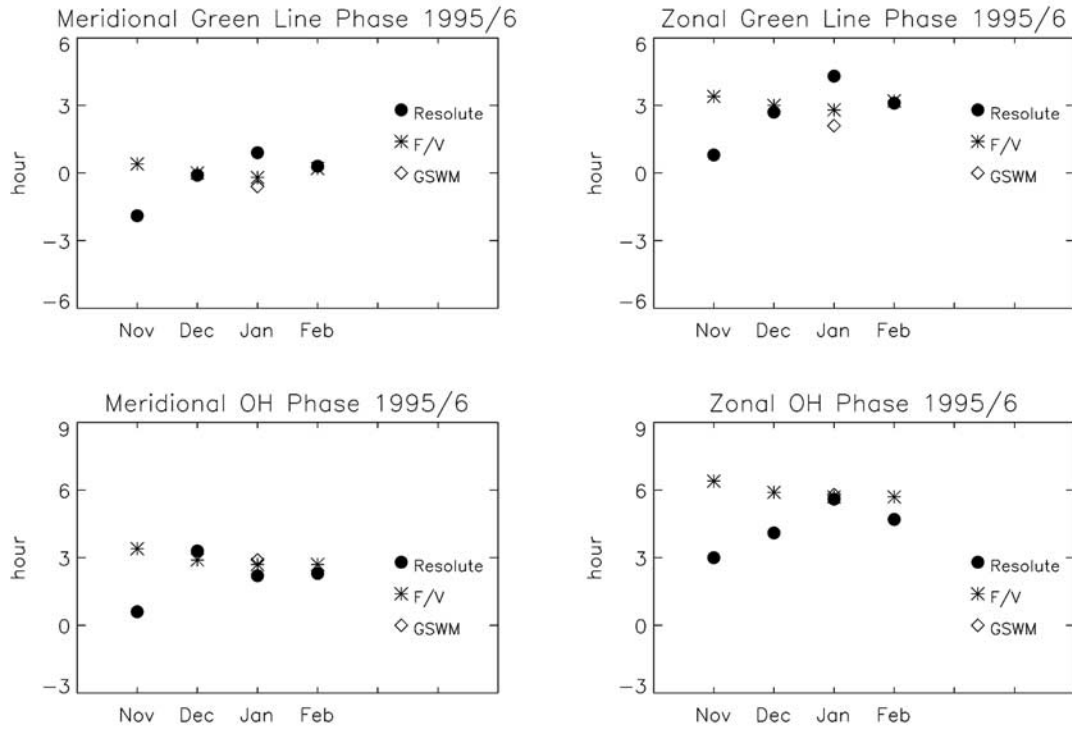
Figure 15. Monthly semidiurnal phases for the 1995/1996 season. The top two plots show the OI (green line) (~97 km) meridional and zonal wind phases and the bottom plots show the OH (~86 km) wind phases. The Resolute data has an error of 0.5 hours. The green line measurements are compared to the Forbes/Vial (F/V) model results at 74°N at 97 km and the GSWM model results at 75°N at 98 km. The OH measurements are compared to the F/V results at 86 km and the GSWM results at 86 km. The green line data were obtained from ERWIN and the OH data were obtained from ERWIN during November and from FPI/CLIO during December–February.
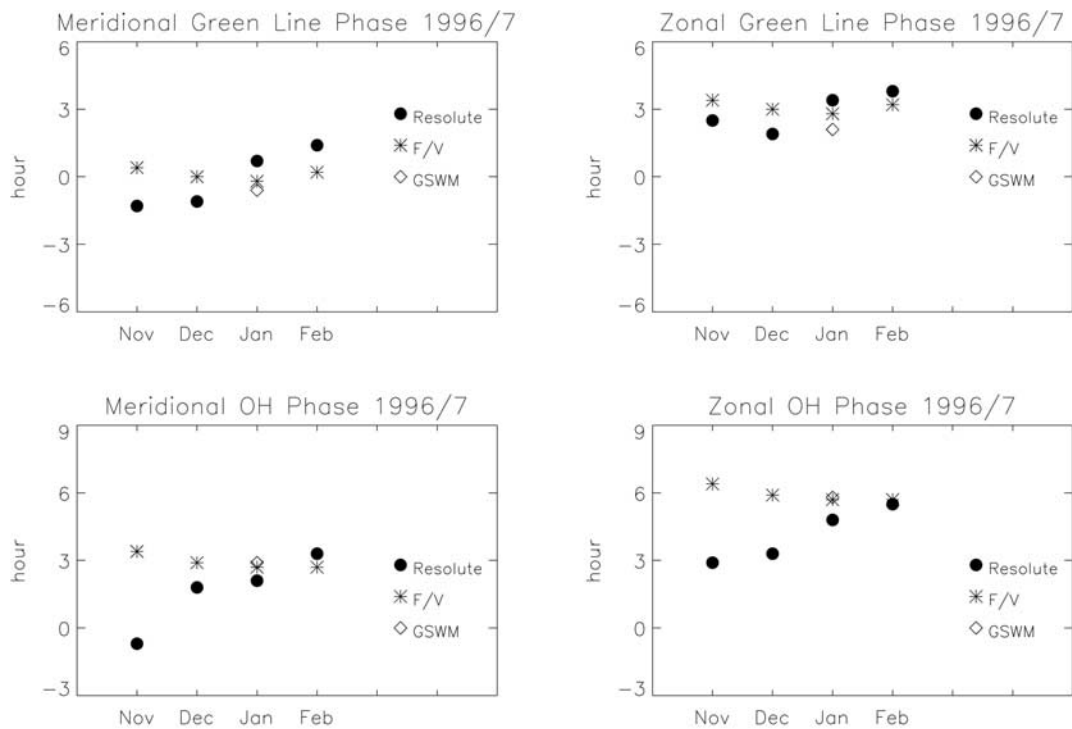

Figure 16. Same as Figure 15 but for the semidiurnal phases during the 1996/1997 season.
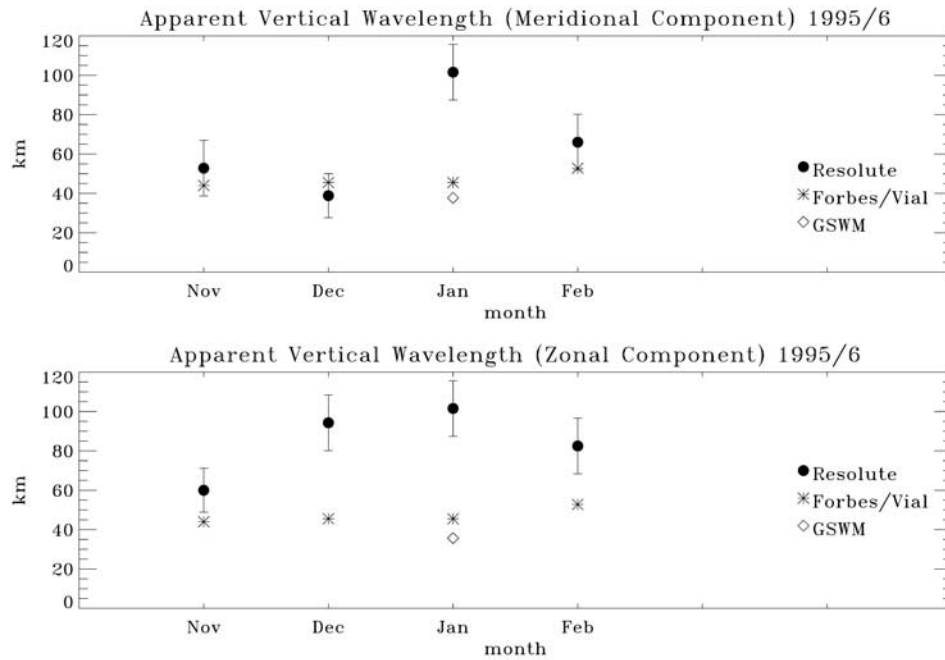
Figure 17. 1995/1996 monthly vertical wavelengths. The top plot shows the meridional component and the lower plot shows the zonal component. The Resolute data, plotted with error bars, are marked with solid circles. The Forbes/Vial model is marked with an asterisk and the GSWM is marked with a diamond.

Figure 18 shows similar results for 1996/1997, except the November meridional data value is extremely high (see caption). Both years display monthly zonal data values that are a factor of two greater than those of the models, yet they behave similarly. November 1996 has an extremely large vertical wavelength in both the meridional and zonal component that may be attributed to other periodic oscillations being present.
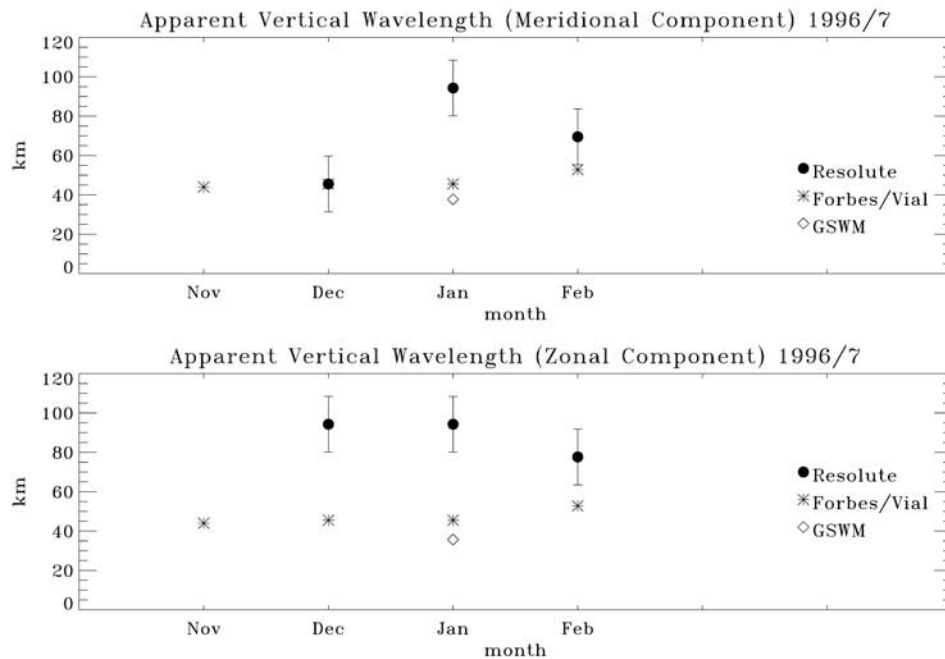
Figure 18. 1996/1997 monthly vertical wavelengths. The top plot is the meridional component and the lower plot is the zonal component. The Resolute data, plotted with error bars, are marked with solid circles. The Forbes/Vial model is marked with an asterisk and the GSWM is marked with a diamond. During November, the apparent vertical wavelength for the meridional component is 220 km and the apparent vertical wavelength for the zonal component is 330 km.

[27] OH and OI observations made at Resolute show that the 12 h component has the characteristics of an upward propagating wave. Both years show similar results in amplitude and phase, except during November 1996, when there were more periodic oscillations present. Daily vertical wavelength calculations show variability throughout the season. Observations compared to the F/V model and the GSWM results indicate the following: 1) the observed OH amplitudes are similar to model results, while the OI observations are about 10 m/s smaller; 2) the observed phases are comparable to the models, except during November and December, when more than one periodic oscillation was significant; and 3) the observed vertical wavelengths are, at times, about a factor of two greater than the models predict.

7. Discussion

[28] Measurements at very high latitudes displaying 12 h and 8 h tides have been reported previously [*Myrabo*, 1984; *Walterscheid et al.*, 1986; *Sivjee et al.*, 1994; *Oznovich et al.*, 1997]. *Walterscheid and Sivjee* [1996] reported an oscillation varying between 12 h and 8 h at Eureka (80°N, 85°W) and suggested that this may be due to the manifestation of source transience or transfer of energy from one wave to another, or possibly limitation in the spectral resolution. *Oznovich et al.* [1997] found no single dominant tide in their winds and intensities at Eureka, yet the most persistent tide in the OH airglow layer was terdiurnal. They concluded that the terdiurnal tide was consistent with an evanescent zonally symmetric tide, which means that the excitation source is spatially localized rather than global. The 12 h tide of the polar mesopause region in winter has been found to be highly variable in amplitude and phase [*Oznovich et al.*, 1997]. The Resolute data also confirm that the amplitudes of the meridional and zonal components of the wind vary [*Fisher et al.*, 1999].

[29] Although the semidiurnal tide is dominant throughout the Resolute data, the 8 h oscillation is transient throughout the winter season. It is unclear if this is the result of the interaction of the 24 h and 12 h wave or if the 8 h wave is a thermal tide. The diurnal tide was not found to be a significant factor in the analysis.

[30] In this paper, an analysis of the tidal behavior of the mesopause winds collected at Resolute was presented. The daily and monthly tidal behavior of the polar mesopause winds were examined over two winter seasons. Results show that quasiperiodic oscillations near tidal frequencies occur regularly at the mesopause. This persistence of the tidal harmonics suggests that the oscillations observed are most likely tidal features. Therefore, it appears that there must be a persistent source for these tidal-like oscillations at the polar latitudes. The semidiurnal tide was found to be the dominant wave during the entire data set. Daily analysis uncovered that the semidiurnal tide at Resolute is variable in phase and amplitude. Long-term analysis of the tides revealed that large-scale variations were found to modulate the semidiurnal characteristics. The mean wind and amplitude varies considerably throughout the winter season. Analysis of the OI winds near 97 km and the OH winds near 86 km show many instances where the semidiurnal oscillation is characteristic of a propagating tide – the OI amplitudes are larger and peak earlier than the OH amplitudes.

[31] Comparisons of the observed winds with numerical predictions indicate discrepancies in amplitudes and phases. Both the GSWM and Forbes/Vial model underestimate the OH wind amplitudes by ~4 m/s. However, the models overestimate the green line amplitudes by ~10 m/s. Generally, the phases between the observations and models differ ~1 h. During November, there is about a 3 h difference, which is probably due to enhanced wave mixing during this month. Calculations of the vertical wavelength of the semidiurnal tide showed that the values are a factor of two greater for the observations than those of the models, yet they behave similarly. It is important to note that the model predicts the migrating components while the observations contain both migrating and non-migrating components.

[32] In the future, the Resolute wind measurements should be combined with the measurements from the upcoming NASA Thermosphere-Ionosphere-Mesosphere, Energetics and Dynamics (TIMED) satellite. On board the satellite will be the TIMED Doppler Interferometer (TIDI), which will provide measurements of vector winds and temperatures from 60–300 km and composition measurements in the mesosphere/lower thermosphere region. TIDI will provide a global coverage, including the poorly measured polar regions. The slow precession rate of the TIMED orbit (3° in longitude per day) allows 24 hours of local time coverage by TIDI in about 60 days using both the ascending and descending portions of the orbit. These satellite measurements will allow wave modes of the tides to be determined. Classical tidal theory (Hough modes) predicts where the wave modes have minima and maxima peaks. The zonal wave number (s) may be determined if measurements are made at numerous locations on a given latitude. The meridional wave number (n) may be determined if measurements are made at numerous locations on a given longitude. If the winds are prescribed by classical wave models, then observations at appropriate spatial positions and local times may provide a measure of the amplitude and phase of the dominant tidal waves. The TIDI measurements can also be used to complement the Resolute data in order to determine if the tides are migrating or non-migrating. To determine if the observed semidiurnal tide is a migrating tide (s = 2), a wind measurement is needed at 180° longitude from Resolute (74.9°N, 94.9°W). A migrating semidiurnal tide should have the same phase at 94.9°W and 274.9°W. Using the wind measurements from TIDI, we can gain a better understanding of the waves near the polar mesopause.

8. Conclusion

[33] Mesopause OH winds were obtained with the FPI/CLIO instrument to examine the daily and monthly variations of the waves (December–March). OH and OI data were obtained from the ERWIN instrument (November–February) for comparison with the FPI during the 1995/1996 and 1996/1997 observing seasons. The tidal analysis of the winds indicates that the mesopause region is dominated by a strong semidiurnal oscillation during the winter season. The significant results of this paper are summarized as follows:

1. Quasiperiodic oscillations near the semidiurnal tidal frequency occur regularly at the mesopause. This persistence of the tidal harmonic suggests that the oscillations

observed are most likely tidal features. Analysis of the daily OH winds reveals that the spectral power is stronger in January than during the other winter months.

2. The 12 h tide is highly variable in amplitude and phase. This may be due to unresolved combinations of tidal frequencies and planetary waves.

3. The phase quadrature relationship between the zonal and meridional semidiurnal components observed near 86 km indicates a propagating tide at this height.

4. The daily mean and tidal components observed near 86 km and 97 km suggest increasing semidiurnal amplitudes with height for both the zonal and meridional components. Phase calculations indicate an upward propagating tide.

5. Comparisons of observed winds with the corresponding theoretical predictions from the GSWM and Forbes/Vial model indicate that the observed monthly semidiurnal amplitudes near 86 km are similar to the model results, while the observations near 97 km are about 10 m/s smaller.

6. The observed monthly semidiurnal phases are comparable to the models, except during November and December, when more than one periodic oscillation was significant. In general, wave mixing is more apparent during November and December than in January and February.

7. Monthly-averaged observed vertical wavelengths of the semidiurnal tide vary from 40–100 km. The observed vertical wavelengths are about a factor of two greater than the models predict. During November 1996, both the meridional and zonal components have extremely large vertical wavelengths (200–300 km). When there is more than one wave mode present, it can result in slight variations in the semidiurnal phase, which results in extremely large vertical wavelengths.

References

Baker, D. J., and A. T. Stair, Rocket measurements of the altitude distribution of the hydroxyl airglow, *Phys. Scr.*, 37, 611–622, 1988.

Fisher, G. M., T. L. Killeen, Q. Wu, P. B. Hays, and J. M. Reeves, Tidal variability of the geomagnetic polar cap mesopause above Resolute Bay, *Geophys. Res. Lett.*, 26, 573–576, 1999.

Fisher, G. M., T. L. Killeen, Q. Wu, J. M. Reeves, P. B. Hays, W. A. Gault, S. Brown, and G. G. Shepherd, Polar cap mesosphere wind observations: Comparisons of simultaneous measurements with a Fabry-Perot interferometer and a field-widened Michelson interferometer, *Appl. Opt.*, 39, 4284–4291, 2000.

Forbes, J. M., and F. Vial, Monthly simulations of the solar semidiurnal tide in the mesosphere and lower thermosphere, *J. Atmos. Terr. Phys.*, 51, 649–661, 1989.

Forbes, J. M., and X. Zhang, Quasi 2-day oscillation of the ionosphere: A statistical study, *J. Atmos. Terr. Phys.*, 59, 1025–1034, 1997.

Forbes, J. M., N. A. Makarov, and Y. I. Portnyagin, First results from the meteor radar at south pole: A large 12-hour oscillation with zonal wavenumber one, *Geophys. Res. Lett.*, 22, 3247–3250, 1995.

Forbes, J. M., Y. I. Portnyagin, N. A. Makarov, S. E. Palo, E. G. Merzlyakov, and X. Zhang, Dynamics of the lower thermosphere over South Pole from meteor radar wind measurements, *Earth Planets Space*, 51, 611–620, 1999.

Gault, W. A., S. Brown, A. Moise, D. Liang, G. Seller, G. G. Shepherd, and J. Wimperis, ERWIN: An E-region wind interferometer, *Appl. Opt.*, 35, 2913–2922, 1996.

Greer, R. G. H., et al., ETON1: A data base pertinent to the study of energy transfer in the oxygen nightglow, *Planet. Space Sci.*, 34, 771–788, 1986.

Hagan, M. E., M. D. Burrage, J. M. Forbes, J. Hackney, and W. J. Randel, GSWM-98: Results for migrating solar tides, *J. Geophys. Res.*, 104, 6813–6827, 1999.

Hays, P. B., Circle to line interferometer optical system, *Appl. Opt.*, 29, 1482–1489, 1990.

Hernandez, G., R. W. Smith, and J. F. Conner, Neutral wind and temperature in the upper mesopause above South Pole, Antarctica, *Geophys. Res. Lett.*, 19, 53–56, 1992a.

Hernandez, G., R. W. Smith, G. J. Fraser, and W. L. Jones, Large-scale waves in the upper mesosphere at Antarctic high latitudes, *Geophys. Res. Lett.*, 19, 1347–1350, 1992b.

Hernandez, G., G. J. Fraser, and W. L. Jones, Mesospheric 12 hour oscillation near South Pole, Antarctica, *Geophys. Res. Lett.*, 20, 1787–1790, 1993.

Hernandez, G., R. Wiens, R. P. Lowe, G. G. Shepherd, G. J. Fraser, R. W. Smith, L. M. LeBlanc, and M. Clark, Optical determination of the vertical wavelength of propagating 12-hour period upper atmosphere oscillations, *Geophys. Res. Lett.*, 22, 2389–2392, 1995.

Hernandez, G., J. M. Forbes, R. W. Smith, Y. Portnyagin, J. F. Booth, and N. Makarov, Simultaneous mesospheric wind measurements near South Pole by optical and meteor radar methods, *Geophys. Res. Lett.*, 23, 1079–1082, 1996.

Lopez-Moreno, J. J., R. Rodrigo, F. Moreno, M. Lopez-Puertas, and A. Molina, Altitude distribution of vibrationally excited states of atmospheric hydroxyl at levels v = 2 to v = 7, *Planet. Space Sci.*, 35, 1029–1038, 1987.

Manson, A. H., C. E. Meek, and G. E. Hal, Correlations of gravity waves and tides in the mesosphere over Saskatoon, *J. Atmos. Terr. Phys.*, 60, 1089–1107, 1998.

Manson, A. H., et al., Seasonal variations of the semidiurnal and diurnal tides in the MLT: Multi-year MF radar observations from 2 to 70N, and the GSWM tidal model, *J. Atmos. Terr. Phys.*, 61, 809–828, 1999.

Myrabo, H. K., Temperature variation at mesopause levels during winter solstice at 78 N, *Planet. Space Sci.*, 37, 249–255, 1984.

Oznovich, I., D. J. McEwen, and G. G. Sivjee, Temperature and airglow brightness oscillations in the polar mesosphere and lower thermosphere, *Planet. Space Sci.*, 43, 1121–1130, 1995.

Oznovich, I., D. J. McEwen, G. G. Sivjee, and R. L. Walterscheid, Tidal oscillations of the Arctic upper mesosphere and lower thermosphere in winter, *J. Geophys. Res.*, 102, 4511–4520, 1997.

Portnyagin, Y. I., J. M. Forbes, N. A. Makarov, E. G. Merzlyakov, and S. Palo, The summertime 12-h wind oscillation with zonal wavenumber s = 1 in the lower thermosphere over the South Pole, *Ann. Geophys.*, 16, 828–837, 1998.

Portnyagin, Y. I., J. M. Forbes, E. G. Merzlyakov, N. A. Makarov, and S. E. Palo, Intradiurnal wind variations observed in the lower thermosphere over the South Pole, *Ann. Geophys.*, 18, 547–554, 2000.

Press, W. H., S. A. Teukolsky, W. T. Vetterling, and B. P. Flannery, *Numerical Recipes*, Cambridge Univ. Press, New York, 1992.

Salah, J. E., W. Deng, and R. R. Clark, Observed dynamical coupling through tidal wave propagation in the mesosphere and lower thermosphere at midlatitudes, *J. Atmos Terr. Phys.*, 59, 641–654, 1997.

Sivjee, G. G., and R. L. Walterscheid, Six-hour zonally symmetric tidal oscillations of the winter mesosphere over the South Pole station, *Planet. Space Sci.*, 42, 447–453, 1994.

Sivjee, G. G., R. L. Walterscheid, and D. J. McEwen, Planetary wave disturbances in the Arctic winter mesopause over Eureka (80N), *Planet. Space Sci.*, 42, 973–986, 1994.

Walterscheid, R. L., and G. G. Sivjee, Very high frequency tides observed in the airglow over Eureka, *Geophys. Res. Lett.*, 23, 3651–3654, 1996.

Walterscheid, R. L., and G. G. Sivjee, Zonally symmetric oscillations observed in the airglow from South Pole Station, *J. Geophys. Res.*, 106, 3645–3654, 2001.

Walterscheid, R. L., G. G. Sivjee, G. Schubert, and R. M. Hamwey, Large amplitude semidiurnal variations in the polar mesosphere: Evidence of a pseudotide, *Nature*, 324, 347–349, 1986.

Wu, J., J. Wang, and P. B. Hays, Performance of a circle-to-line optical system for a Fabry-Perot interferometer: A laboratory study, *Appl. Opt.*, 33, 7823–7828, 1994.

S. Brown, Centre for Research in Earth and Space Technology, Toronto, Ontario, Canada M3J3K1.

G. M. Fisher, Atmospheric Policy Program, American Meteorological Society, 1120 G Street, NW, Suite 800, Washington, DC 20005, USA.

W. A. Gault and G. G. Shepherd, Centre for Research on Earth and Space Sciences, York University, Toronto, Ontario, Canada M3J1P3.

T. L. Killeen and Q. Wu, National Center for Atmospheric Research, Boulder, CO 80307, USA.

R. J. Niciejewski, Space Physics Research Laboratory, University of Michigan, Ann Arbor, MI 48109, USA.